Direct Visualization of Hyaluronic Acid Polymer Chain by Self-Assembled One-Dimensional Array of Gold Nanoparticles

Haeshin Lee, Seung Ho Choi, and Tae Gwan Park*

Department of Biological Sciences, Korea Advanced Institute of Science and Technology, Daejeon, South Korea 305-701

Received September 5, 2005
Revised Manuscript Received November 10, 2005

Metal nanoparticles have been widely used for medical diagnostics, sensor, and biological imaging.[1−3] In particular, gold nanoparticles have been a subject to study the relationship between electrooptical properties and physical structures.[4] An unusual characteristic represented by surface plasma resonance (SPR) occurs when the size of metal particles (r) becomes quite small relative to the wavelength of light ($r/\lambda \ll 1$). The optophysical properties are tailored by sizes and interparticle interactions. Examples of particle interactions include controlled spatial arrays by utilizing programmed self-assembly of biomacromolecules[5] or nanophase separation of synthetic polymers.[6] Synthetic polymers such as diblock copolymers have been used as templates for nanoparticle assembly by providing a wide range of contour lengths by molecular weight and side chain functionalities. An example of side chain induced gold nanoparticle array was reported by Zehner et al. in which they utilized specific binding between gold and phenyl groups of poly(styrene-*block*-methyl methacrylate) via $\pi-\pi^*$ interactions.[7] In addition, highly ordered assembly of nanoparticles has been obtained by combination of different interactions from diverse polymer architectures.[6,8] The use of synthetic polymers is advantageous over lithographic approaches[9] in that it can be easily scaled up for the future manufacture of single molecule electronic circuits. However, polymer-based systems are often not compatible with aqueous solvents hampering biological applications.

Herein we report to fabricate one-dimensional array of gold nanoparticles, in which their self-assembly structures were dictated by a naturally occurring biopolymer, hyaluronic acid (HA).[10] HA, a linear polysaccharide chain found predominantly in the extracellular matrix (ECM) of connective tissues, was used to provide a template for gold nanoparticle assembly. HA has disaccharide AB-type repeating units composed of *N*-acetylglucosamine and glucuronic acid. They are linked by a β-glycosidic bond (Figure 1A). It is extremely difficult to chemically synthesize such a $(AB)_n$-type polymer with several thousand repeats ($n > 1000$), but biology does it with ease. In glucuronic acid, a carboxyl group is attached at the fifth carbon of the sugar ring (Figure 1A). Thus, a precise spatial distribution of carboxyl groups is naturally achieved at a template level, and the resulting distance between carboxyl groups is about 1 nm when stretched. It was postulated that thiolated HA in the place of carboxylic acid groups can be used as a template to spatially control one-dimensional array of gold nanoparticles (∼20 nm in diameter in our study) by gold−thiol interactions. The thiol groups in the HA backbone were introduced by chemical modification of the carboxyl groups. The 1 nm spatial distribution of acid groups allows us to have a certain degree of freedom over the yield of chemical modification: the partial modification, at best 10−20 conjugation percent, is a satisfactory level to achieve a gold nanoparticle array considering the size of nanoparticles used in our study (∼20 nm).

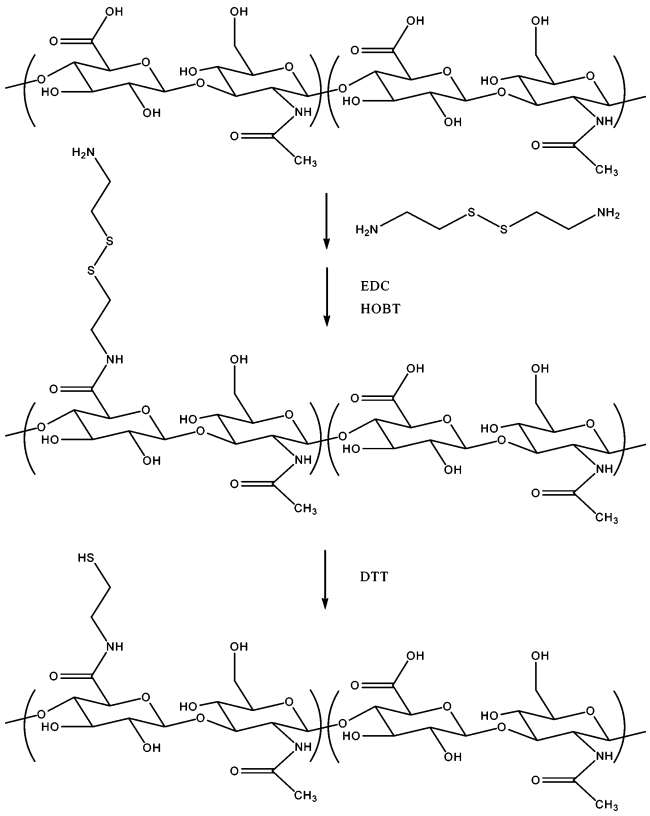

Figure 1. Chemical introduction of thiol groups on hyaluronic acid. Carboxyl groups in HA were reacted with cystamine molecules by activation with EDC and HOBT. Reduction of cystamine by DTT resulted in free thiol groups in the HA backbone.

Carboxyl groups in HA were functionalized to thiol groups by a simple two-step reaction scheme which is depicted in Figure 1. First, the carboxylic acid groups of HA were chemically activated by 1-ethyl-3-(3-dimethylaminopropyl)-carbodiimide hydrochloride (EDC) and 1-hydroxybenzotriazole (HOBT) and subsequently conjugated with cystamine dihydrochloride at pH 6.8 for 12 h. The reaction mixture was exhaustively dialyzed by a molecular weight cutoff 3500 dialysis membrane against distilled deionized water (DDW). Second, dithiothreitol (DTT) was added to reduce disulfide bonds of HA-conjugated cystamines and subsequently increased pH to 8.5. After the mixture was stirred for overnight, the solution pH was dropped to 3.5 and NaCl was added (5% w/v). Subsequently, thiolated HA was precipitated by excess ethanol and redissolved in DDW, which was freeze-dried for storage. Thiol modification was about 72% as determined by the ^{1}H NMR data. This degree of modification resulted in ∼1.3 nm thiol−thiol distance on average, which can be regarded as a sufficient level for nanoparticle assembly. The gold nanoparticles used in this report (∼20 nm) were synthesized by well-known trisodium citrate methods.[11] Briefly, $HAuCl_4$ solution (0.01%, w/v) was boiled for 15 min with vigorous stirring. The 1% (w/v) trisodium citrate was added to make a gold nanoparticle solution, which resulted in an indicative color change from purple red to red. The reaction was allowed to continue for 15

* To whom correspondence should be addressed: Tel +82-42-869-2621; Fax +82-42-869-2610; e-mail tgpark@kaist.ac.kr.

10.1021/ma051929c CCC: $33.50
Published on Web 11/24/2005

min, and then the solution was cooled to room temperature. Equal volumes of HA and gold nanoparticle solutions were prepared, and the nanoparticles were added to the HA solution in a dropwise manner (the thiolated HA in excess with a weight ratio of 20/1). The mixture was stirred for 1 h at room temperature. It should be emphasized that our assembly procedure was performed in aqueous conditions due to the water-soluble and biocompatible properties of HA, which has been used as biomaterials for tissue engineering scaffolds and hydrogels.[12]

Transmission electron microscopy (TEM) was used to show the morphology of the HA/Au nanoparticle array. Gold nanoparticles were surprisingly well aligned along the single chain of HA, in which the binding was driven by the strong affinity between gold surface and sulfur moieties in HA (Figure 2A). The calculated contour length of the polymer chain was ~1.8 μm, which fell reasonably into the theoretical HA chain length of 1.4−4.7 μm (0.3−1 MDa). The calculation was performed in Adobe Photoshop 6.0 by fragmenting the TEM image into linear arrays and calculated the lengths by pixel data. These data suggested that the entire HA polymer chain was almost perfectly visualized by one-dimensional array of gold nanoparticles. Detailed nanoparticle array patterns revealed two interesting features. (1) Double-chain arrays of nanoparticles on both side of chains were often detected (Figure 2B). This indicated that the high degree of substitution (72%) resulted in the exposure of free thiols on both side of chains, which represented as a dual-line of nanoparticle array. (2) Local aggregation of nanoparticles was also visualized. This might be due to the intramolecular chain−chain overlap caused by backbone flexibility as well as intrinsic nanoparticle aggregations (Figure 2C). These results challenged us toward further study of optimizing the degree of chemical modification on the polymer backbones, the size and concentrations of nanoparticles, and the selection of colloidal stabilizers. It should be noted that the initial concentration of HA and the stoichiometric balance (excess amount of nanoparticles) are the two utmost important factors in generating such a well-aligned gold particle structure along the HA chain. Clustered gold nanoparticles were often visualized due to the accelerated chain cross-linking by thiol oxidation at a high concentration of HA. The partial intramolecular cross-linking was unavoidable even in the presence of DTT. During the visualization, no gold colloidal instability was observed except for the cluster alignment of nanoparticles directed by the intramolecular thiol oxidation. Aggregated gold nanoparticles were densely localized at the core of the oxidized HA chain, which is not an indication of colloidal instability (Figure 2D).

HA-mediated one-dimensional array of gold nanoparticles showed interesting optical properties. It exhibited two distinct peaks: 520 and 677 nm (Figure 3). The short wavelength peak was from the plasmon resonance effect of well-dispersed monomeric gold particles (λ_{max} = 520 nm). The extent of visible shift (157 nm) was unexpectedly larger than those reported in previous studies of gold nanoparticle assembly. Dendrimer-mediated spatial control of gold nanoparticles exhibited 66 nm red shift from well-dispersed particles in solution (526 nm) by 0.6 nm interparticle distance alignment. An additional 18 nm red shift was observed when a solid thin film of the same nanoparticles was prepared (610 nm).[8] Gold nanoparticles embedded in cationic polymer, poly(ethylenimine) (PEI), also showed a red shift up to 620 nm.[6] These results were caused by the change of dielectric environments and polarized dipole−dipole interactions, which have shown a relatively small extent

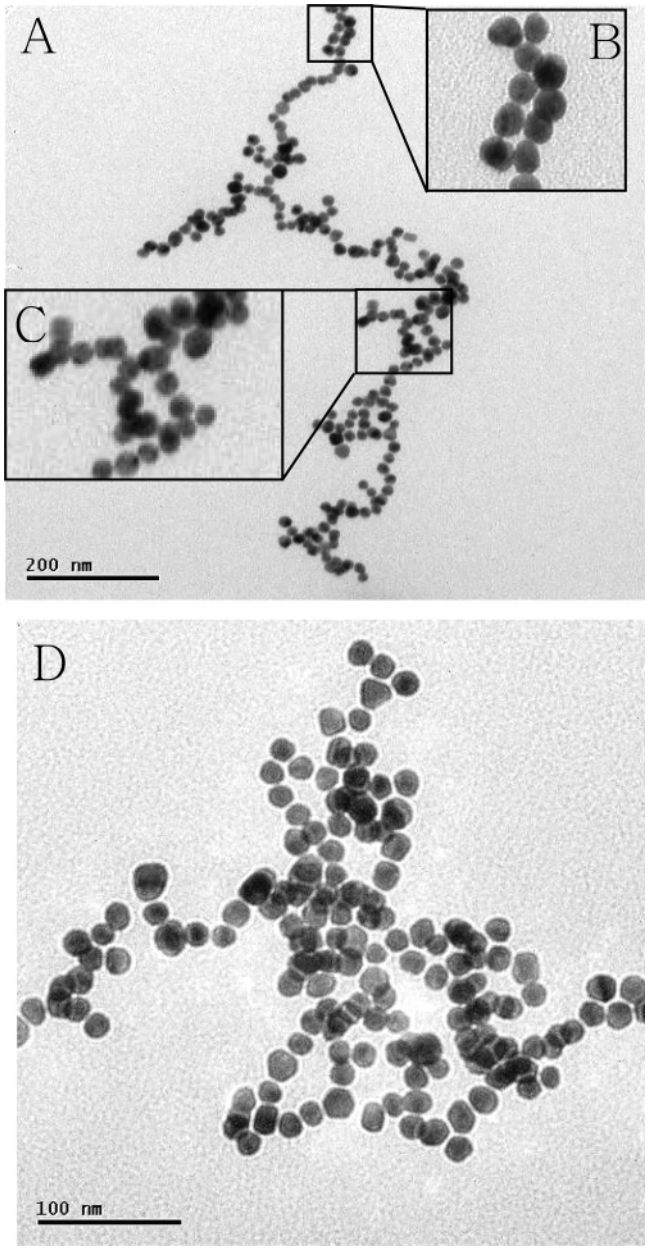

Figure 2. Transmission electron microscopic (TEM) images of thiolated hyaluronic acid/gold nanoparticle complexes. (A) One-dimensional array of gold nanoparticles on hyaluronic acid backbone via interactions between thiol groups in HA and gold surface. Detail zoom-in representations of gold nanoparticle arrays: (B) a double-chain array and (C) local nanoparticle aggregations. (D) Cluster array of gold nanoparticles onto intramolecular cross-linked hyaluronic acid chains via disulfide bond formations.

of red shift compared to our results (677 nm). This longer wavelength shift, therefore, might be due to the additional effect of anisotropic longitudinal resonance along the aligned particles.[13] Considering a purely longitudinal resonance effect, our complex corresponded to the aspect ratio of ~2.8. Thus, the observed optical property seemed to be combined effects of anisotropic (longitudinal) resonance and dielectric and/or dipole interactions. It should be noted that the HA/nanoparticle complexes were very stable, maintaining the same optical property for more than 10 days at room temperature. This stability is due to the strong binding between gold and sulfur group (40−70 kcal/mol),[14] which is almost equivalent to covalent bond strength by in AFM (~1.4 nN).[15]

CDV

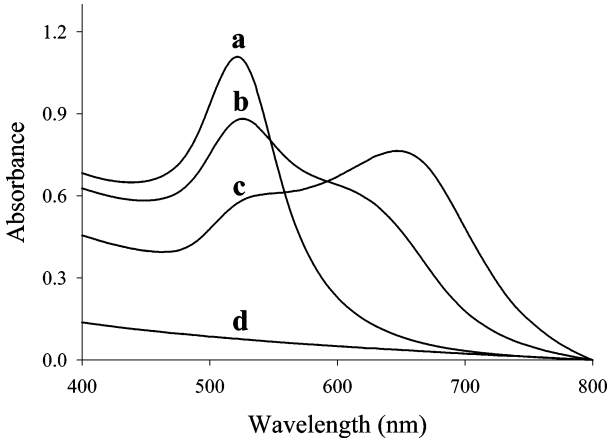

Figure 3. Surface plasma resonance spectra of hyaluronic acid-induced array of gold nanoparticles: (A) water-dispersed gold nanoparticles, (B, C) addition of thiolated hyaluronic acid (1 and 3.2 mg), and (D) hyaluronic acid alone. Fully assembled nanoparticles showed two resonance peaks, 520 and 677 nm.

In conclusion, this study represents that one-dimensional gold nanoparticle array could be fabricated using biomacromolecules i.e., thiolated hyaluronic acid as a template. Direct visualization of a HA chain structure could be possible by the aligned gold nanoparticles in aqueous solution.

Acknowledgment. Authors deeply thank Dr. Rongchao Jin, Mason Gruffy, Sungho Park, and Shunji Egusa for their insightful discussions. This study was supported by a grant (0405-MN01-0604-0007) from the Ministry of Health and Welfare, Korea.

References and Notes

(1) (a) Hayat, M. A. *Colloidal Gold: Principles, Methods, Applications*; Academic Press: San Diego, CA, 1989. (b) Kreibig, U.; Vollmer, M. *Optical Properties of Metal Clusters*; Springer: Berlin, 1995.
(2) (a) Elghanian, R.; Storhoff, J. J.; Mucic, R. C.; Letsinger, R. L.; Mirkin, C. A. *Science* **1997**, *277*, 1078−1081. (b) Nath, N.; Chilkoti, A. *J. Fluoresc.* **2004**, *14*, 377−388. (c) He, L.; Musick, M. D.; Nicewarner, S. R.; Salinas, F. G.; Natan, M. J.; Keating, C. D. *J. Am. Chem. Soc.* **2000**, *122*, 9071−9073.
(3) Taton, T. A.; Mirkin, C. A.; Letsinger, R. L. *Science* **2000**, *289*, 1757−1760.
(4) Goia, D. V.; Matijevic, E. *Colloids Surf., A* **1999**, *146*, 139−152.
(5) (a) Douglas, T.; Young, M. *Nature (London)* **2002**, *393*, 152−155. (b) Keren, K.; Krueger, M.; Gilad, R.; Ben-Yoseph, G.; Sivan, U.; Braun, E. *Science* **2002**, *297*, 72−75.
(6) Schmid, G.; Baumle, M.; Beyer, N. *Angew. Chem., Int. Ed.* **2000**, *39*, 181−183.
(7) Zehner, R. W.; Lopes, W. A.; Morkved, T. L.; Jaeger, H.; Sita, L. R. *Langmuir* **1998**, *14*, 241−244.
(8) Srivastava, S.; Frankamp, B. L.; Rotello, V. M. *Chem. Mater*. **2005**, *17*, 487−490.
(9) Mendes, P. M.; Jacke, S.; Critchley, K.; Plaza, J.; Chen, Y.; Nikitin, K.; Palmer, R. E.; Preece, J. A.; Evans, S. D.; Fitzmaurice, D. *Langmuir* **2004**, *20*, 3766−3768.
(10) Lee, J. Y.; Spicer, A. P. *Curr. Opin. Cell Biol*. **2000**, *12*, 581−586.
(11) Turkevitch, J.; Stevenson, P. C.; Hillier, J. *Discuss. Faraday Soc.* **1951**, *11*, 55−75.
(12) (a) Burdick, J. A.; Chung, C.; Jia, X.; Randolph, M. A.; Langer, R. *Biomacromolecules* **2005**, *6*, 386−391. (b) Hahn, S. K.; Jelacic, S.; Maier, R. V.; Stayton, P. S.; Hoffman, A. S. *J. Biomater. Sci., Polym. Ed.* **2004**, *15*, 1111−1119. (c) Yoo, H. S.; Lee, E. A.; Yoon, J. J.; Park, T. G. *Biomaterials* **2005**, *26*, 1925−1933. (d) Kim, M. R.; Park, T. G. *J. Controlled Release* **2002**, *80*, 69−77.
(13) (a) Nikoobakht, B.; El-Sayed, M. A. *Chem. Mater*. **2003**, *15*, 1957−1962. (b) Yu, Y.-Y.; Chang, S.-S.; Lee, C.-L.; Wang, C. R. C. *J. Phys. Chem. B* **1997**, *101*, 6661−6664.
(14) Letardi, S.; Cleri, F. *J. Chem. Phys*. **2004**, *120*, 10062−10068.
(15) Grandbois, M.; Beyer, M.; Rief, M.; Clausen-Schaumann, H.; Gaub, H. E. *Science* **1999**, *283*, 1727−1730.

MA051929C